Audio Engineering Society

Convention Paper

Presented at the 124th Convention
2008 May 17–20 Amsterdam, The Netherlands

The Theory of Wave Field Synthesis Revisited

Sascha Spors[1], Rudolf Rabenstein[2], and Jens Ahrens[1]

[1] *Deutsche Telekom Laboratories, Berlin University of Technology, Ernst-Reuter-Platz 7, 10587 Berlin, Germany*

[2] *Multimedia and Signal Processing, University of Erlangen-Nuremberg, Cauerstrasse 7, 91058 Erlangen, Germany*

Correspondence should be addressed to Sascha Spors (`Sascha.Spors@telekom.de`)

ABSTRACT

Wave field synthesis is a spatial sound field reproduction technique aiming at authentic reproduction of auditory scenes. Its theoretical foundation has been developed almost 20 years ago and has been improved considerably since then. Most of the original work on wave field synthesis is restricted to the reproduction in a planar listening area using linear loudspeaker arrays. Extensions like arbitrarily shaped distributions of secondary sources and three-dimensional reproduction in a listening volume have not been discussed in a unified framework so far. This paper revisits the theory of wave field synthesis and presents a unified theoretical framework covering arbitrarily shaped loudspeaker arrays for two- and three-dimensional reproduction. The paper additionally gives an overview on the artifacts resulting in practical setups and briefly discusses some extensions to the traditional concepts of WFS.

1. INTRODUCTION

Wave field synthesis (WFS) is a spatial sound field reproduction technique that utilizes a high number of loudspeakers to create a virtual auditory scene over a large listening area. It overcomes some of the limitations of stereophonic reproduction techniques, like e. g. the sweet-spot.

A first concept, of what is nowadays known as WFS, was presented by Snow et al. [1] more than 50 years ago. However, technical constraints prohibited the employment of a high number of loudspeakers for sound reproduction. The authors therefore employed only some few loudspeakers and essentially laid the theoretical fundament for stereophonic techniques. It took quite some time until the initial ideas of Snow have been taken up again.

The theoretical framework of WFS was initially formulated by Berkhout et al. at the Delft University of Technology almost 20 years ago [2]. However, it seems that the term 'wave field synthesis' has been mentioned the first time some years later [3]. Also around that time first laboratory setups of WFS sys-

tems have been realized. Sound reproduction using WFS has gained quite some attraction in the spatial audio research community. Besides various research projects, like e. g. the EC IST funded project CARROUSO [4], also a number of PhD theses have been written in the context of WFS so far [5, 6, 7, 8, 9, 10, 11, 12, 13, 14]. General overviews on WFS can be found e. g. in [15, 16, 17, 18, 19, 20, 21, 22, 23, 24]. Most of the original work on WFS considers the reproduction in a planar listening area (two-dimensional wave field synthesis), using a linear distribution of loudspeakers. Although the theory of WFS has been extended in various aspects, topics like arbitrarily shaped distributions of loudspeakers and three-dimensional reproduction have gained only little attention so far. This paper will revisit the physical background of WFS and will present a unified framework that covers these aspects.

For this purpose our paper begins in Section 2 with the generic formulation of the underlying physical problem using the Kirchhoff-Helmholtz integral. It will be shown how to derive a formulation from this fundamental principle that is applicable in practical setups. Section 3 specializes the generic theory of WFS developed so far, to the case of three-dimensional reproduction in a volume. The three-dimensional formulation serves as basis for the description of the conventional two-dimensional WFS schemes introduced in Section 4. In order to span the bridge to the traditional theory of WFS, the loudspeaker driving functions derived within this paper will be compared to the classical WFS literature. Besides revisiting the foundations of WFS, Section 5 will give an overview on the artifacts resulting from further assumptions and simplifications performed in practical setups. Finally some extensions to WFS will be discussed in Section 6.

The following conventions are used throughout this paper: For scalar variables lower case denotes the time domain, upper case the temporal frequency domain. The temporal frequency variable is denoted by $\omega = 2\pi f$. Vectors are denoted by lower case boldface. The three-dimensional position vector in Cartesian coordinates is given as $\mathbf{x} = [x\ y\ z]^T$. Two-dimensional wave fields are also considered within this paper. The required reduction in dimensionality is performed by assuming that the reproduced wave field is independent from the z-coordinate, e. g. $P(x, y, z, \omega) = P(x, y, \omega)$.

2. BASIC THEORY

This section introduces the basic theory of wave field synthesis.

2.1. The Kirchhoff-Helmholtz Integral

A loudspeaker system surrounding the listener can be regarded as an inhomogeneous boundary condition for the wave equation. This will be illustrated in the following.

The solution of the homogeneous wave equation for a bounded region V with respect to inhomogeneous boundary conditions is given by the Kirchhoff-Helmholtz integral [25]

$$P(\mathbf{x},\omega) = -\oint_{\partial V} \Big(G(\mathbf{x}|\mathbf{x}_0,\omega)\, \frac{\partial}{\partial \mathbf{n}} P(\mathbf{x}_0,\omega) - P(\mathbf{x}_0,\omega)\, \frac{\partial}{\partial \mathbf{n}} G(\mathbf{x}|\mathbf{x}_0,\omega) \Big)\, dS_0 \ , \quad (1)$$

where $P(\mathbf{x},\omega)$ denotes the pressure field inside a bounded region V enclosed by the boundary ∂V ($\mathbf{x} \in V$), $G(\mathbf{x}|\mathbf{x}_0,\omega)$ a suitable chosen Green's function, $P(\mathbf{x}_0,\omega)$ the acoustic pressure at the boundary ∂V ($\mathbf{x}_0 \in \partial V$) and $\mathbf{n}$ the inward pointing normal vector of ∂V. The abbreviation $\frac{\partial}{\partial \mathbf{n}}$ denotes the directional gradient in direction of the normal vector $\mathbf{n}$. For instance $\frac{\partial}{\partial \mathbf{n}} P(\mathbf{x}_0,\omega)$ is

$$\frac{\partial}{\partial \mathbf{n}} P(\mathbf{x}_0,\omega) = \langle \nabla P(\mathbf{x},\omega), \mathbf{n}(\mathbf{x}_0) \rangle \Big|_{\mathbf{x}=\mathbf{x}_0} \ , \quad (2)$$

where $\langle \cdot, \cdot \rangle$ denotes the scalar product of two vectors. The wave field $P(\mathbf{x},\omega)$ outside of V is zero and V is assumed to be source-free. Figure 1 illustrates the geometry.

The Green's function $G(\mathbf{x}|\mathbf{x}_0,\omega)$ represents the solution of the inhomogeneous wave equation for excitation with a spatio-temporal Dirac pulse at the position $\mathbf{x}_0$. It has to fulfill the homogeneous boundary conditions imposed on ∂V. For sound reproduction typically free-field propagation within V is assumed. This means that V is free of any objects and that the boundary ∂V does not restrict propagation. The Green's function is then given as the free-field solution of the wave equation and is referred to as *free-field Green's function* $G_0(\mathbf{x}|\mathbf{x}_0,\omega)$. The free-field Green's function can be interpreted as the spatio-temporal transfer function of a monopole placed at the point $\mathbf{x}_0$ and its directional gradient as the spatio-temporal transfer function of a dipole

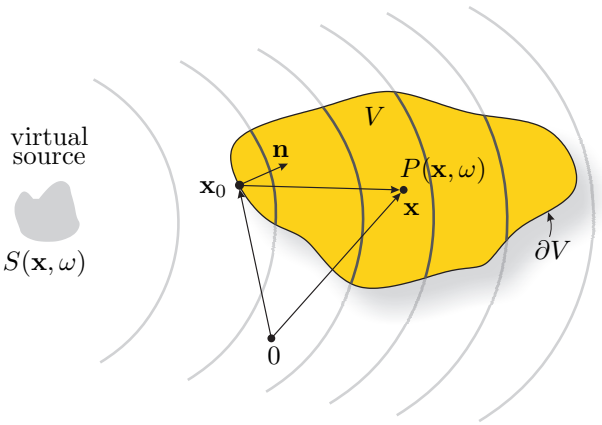

Fig. 1: Illustration of the geometry used for the Kirchhoff-Helmholtz integral (1).

at the point $\mathbf{x}_0$, whose main axis points towards $\mathbf{n}$. Equation (1) states that the wave field $P(\mathbf{x},\omega)$ inside V is fully determined by the pressure $P(\mathbf{x},\omega)$ and its directional gradient on the boundary ∂V. If the Green's function is realized by a continuous distribution of appropriately driven monopole and dipole sources which are placed on the boundary ∂V, the wave field within V is fully determined by these sources. This principle can be used for sound reproduction as will be illustrated in the following. In this context the monopole and dipole sources on the boundary are referred to as (monopole/dipole) *secondary sources*.

For authentic sound field reproduction it is desired to reproduce the wave field $S(\mathbf{x},\omega)$ of a virtual source inside a limited area (listening area) as closely as possible. In the following, the listening area is assumed to be the bounded region V (see Fig. 1). Concluding the considerations given so far, authentic sound field reproduction can be realized if a distribution of secondary monopole and dipole sources on the boundary ∂V of the listening area V are driven by the directional gradient and the pressure of the wave field of the virtual source $S(\mathbf{x},\omega)$, respectively. Thus $P(\mathbf{x}_0,\omega)$ in Eq. (1) is given by the values of $S(\mathbf{x},\omega)$ on ∂V. The wave field $P(\mathbf{x},\omega)$ inside the listening area V is then equal to the wave field $S(\mathbf{x},\omega)$ of the virtual source. The Kirchhoff-Helmholtz integral and its interpretation given above lay the theoretical foundation for WFS and other massive multichannel sound reproduction systems.

It is desirable for a practical implementation to discard one of the two types of secondary sources that the Kirchhoff-Helmholtz integral employs. Typically the dipole sources are removed, since monopole sources can be realized reasonably well by loudspeakers with closed cabinets. According to [25] two different techniques exist to derive monopole only versions of the Kirchhoff-Helmholtz integral: the simple source approach and a modification of the free-field Green's function used in the Kirchhoff-Helmholtz integral. These two approaches will be discussed in the following two subsections.

2.2. Simple Source Approach

The dipole secondary sources in the Kirchhoff-Helmholtz integral can be discarded by considering two equivalent but spatially disjunct problems. The simple source approach is derived by constructing an exterior and separately an interior problem with respect to the boundary ∂V and linking both problems by requiring that the pressure is continuous and the directional gradient is discontinuous at the boundary ∂V [25]. This procedure results in

$$P(\mathbf{x},\omega) = \oint_{\partial V} \mu(\mathbf{x}_0,\omega)\, G_0(\mathbf{x}|\mathbf{x}_0,\omega)\, dS_0 \,. \qquad (3)$$

Equation (3) states that a distribution of monopole sources on ∂V driven by $\mu(\mathbf{x}_0,\omega)$ fully determines the wave field $P(\mathbf{x},\omega)$ within and outside of V. Note, that contrary to the Kirchhoff-Helmholtz formulation the wave field outside of V will not be zero in this case.

It is stated in [25] that the simple source approach delivers the same results as the Kirchhoff-Helmholtz formulation when considering either an interior or exterior problem. Sound reproduction can be regarded as interior problem. The source strength $\mu(\mathbf{x}_0,\omega)$ is given by the underlying physical problem which satisfies the stated boundary conditions. For authentic sound field reproduction it is required that the field $P(\mathbf{x},\omega)$ within V is equal to the wave field of the virtual source $S(\mathbf{x},\omega)$. The appropriate secondary source strength $\mu(\mathbf{x}_0,\omega)$ can be derived by constructing an exterior field that satisfies the required boundary conditions. In general this will only be possible by considering special geometries of the secondary source contour ∂V.

In higher-order Ambisonics [26, 27], and other reproduction techniques [28, 29, 30] which are inherently

based on the simple source approach, Eq. (3) is explicitly solved with respect to $\mu(\mathbf{x}_0, \omega)$. This is typically performed by expanding the respective wave fields using orthogonal wave field expansions. The simple source formulation (3) ensures that a unique solution for the secondary source strength $\mu(\mathbf{x}_0, \omega)$ exists.

2.3. Elimination of Dipole Secondary Sources in WFS

The second term in the Kirchhoff-Helmholtz integral (1), representing the dipole secondary sources, can be discarded by modifying the Green's function used in the Kirchhoff-Helmholtz integral [25]. The modified Green's function $G_\mathrm{N}(\mathbf{x}|\mathbf{x}_0, \omega)$ has to obey the following condition

$$\frac{\partial}{\partial \mathbf{n}} G_\mathrm{N}(\mathbf{x}|\mathbf{x}_0, \omega)\Big|_{\mathbf{x}_0 \in \partial V} = 0 \,, \tag{4}$$

in order to eliminate the dipole secondary sources. Condition (4) formulates a homogeneous Neumann boundary condition imposed on ∂V. The modified Green's function is typically termed Neumann Green's function. As a consequence of the condition given by Eq. (4), the boundary ∂V will be implicitly modeled as an acoustically rigid surface for the secondary sources. The desired Neumann Green's function $G_\mathrm{N}(\mathbf{x}|\mathbf{x}_0, \omega)$ can be derived by adding a suitable homogeneous solution (with respect to the region V) to the free-field Green's function $G_0(\mathbf{x}|\mathbf{x}_0, \omega)$. The explicit form of the Neumann Green's function depends on the geometry of the boundary ∂V. A closed form solution can only be found for rather simple geometries like spheres and planar boundaries. Additionally, the such derived Neumann Green's function has to be realized by physically existing secondary sources. Depending on the explicit form of the Neumann Green's function such secondary sources may be hard to realize in practice.

In the context of WFS linear secondary source contours have been considered mainly so far. A suitable Neumann Green's function for a planar/linear boundary ∂V is given by [25]

$$G_\mathrm{N}(\mathbf{x}|\mathbf{x}_0, \omega) = G_0(\mathbf{x}|\mathbf{x}_0, \omega) + G_0(\mathbf{x}_\mathrm{m}(\mathbf{x})|\mathbf{x}_0, \omega) \,. \tag{5}$$

A solution fulfilling Eq. (4) is given by choosing the receiver point $\mathbf{x}_\mathrm{m}(\mathbf{x})$ as the point $\mathbf{x}$ mirrored at the planar boundary ∂V at the position $\mathbf{x}_0$. Note, that due to the specialized geometry $|\mathbf{x} - \mathbf{x}_0| = |\mathbf{x}_\mathrm{m} - \mathbf{x}_0|$ and thus [24]

$$G_\mathrm{N}(\mathbf{x}|\mathbf{x}_0, \omega) = 2\, G_0(\mathbf{x}|\mathbf{x}_0, \omega) \,. \tag{6}$$

Hence, in this special case $G_\mathrm{N}(\mathbf{x}|\mathbf{x}_0, \omega)$ is equal to a point source with double strength.

Introducing $G_\mathrm{N}(\mathbf{x}|\mathbf{x}_0, \omega)$ into the Kirchhoff-Helmholtz integral for a planar geometry derives the first Rayleigh integral, which is the basis for the traditional derivation of WFS [2, 5, 6, 7]. However, this theoretical basis holds only for linear/planar secondary source distributions. In the following an extension to arbitrarily shaped secondary source contours will be developed.

2.4. Extension to Arbitrarily Shaped Contours

It is assumed that Eq. (5) holds also approximately for other geometries. In this case the receiver point $\mathbf{x}_\mathrm{m}$ is chosen as the point $\mathbf{x}$ mirrored at the tangent to the boundary ∂V at the position $\mathbf{x}_0$. The elimination of the secondary dipole sources for an arbitrary secondary source contour ∂V has two consequences:

1. the wave field outside of V will not be zero, and
2. the reproduced wave field will not match the virtual source field exactly within V.

The first consequence implies that the boundary ∂V has to be convex, so that no contributions from the wave field outside of the listening area V propagate back into the listening area. The second is a consequence of approximating the Neumann Green's function for arbitrary geometries using the solution given by Eq. (5). As mentioned before, the boundary ∂V will be implicitly modeled as rigid boundary. The appropriate Neumann Green's function for a particular geometry compensates inherently for these reflections. Using the Neumann Green's function Eq. (5) for bend secondary source contours leads to artifacts in the reproduced wave field. The most prominent are that the reproduction of the desired wave field will be superimposed by undesired reflections. These artifacts can be attenuated by a modification of the driving function, as will be illustrated in the following.

The main energy of the undesired reflections is reproduced by those secondary sources where the local propagation direction of the virtual wave field does

not coincide with the normal vector $\mathbf{n}$ of the secondary source. Since we are free to choose the secondary sources used for reproduction, these undesired reflections can be attenuated by muting those secondary sources which reproduce the reflections. Following this concept, the reproduced wave field reads

$$P(\mathbf{x},\omega) = - \oint_{\partial V} 2a(\mathbf{x_0}) \frac{\partial}{\partial \mathbf{n}} S(\mathbf{x}_0,\omega)\, G_0(\mathbf{x}|\mathbf{x}_0,\omega)\, dS_0 \;, \quad (7)$$

where $a(\mathbf{x_0})$ denotes a suitably chosen window function. This function takes care that only those secondary sources are active where the local propagation direction of the virtual source at the position $\mathbf{x_0}$ has a positive component in direction of the normal vector $\mathbf{n}$ of the secondary source at that position. It was proposed in [31, 32] to formulate this condition analytically on basis of the acoustic intensity vector

$$a(\mathbf{x}_0) = \begin{cases} 1 & \text{, if } \langle \bar{\mathbf{I}}_\mathrm{S}(\mathbf{x}_0,\omega), \mathbf{n}(\mathbf{x}_0)\rangle > 0, \\ 0 & \text{, otherwise.} \end{cases} \quad (8)$$

The time averaged acoustic intensity vector $\bar{\mathbf{I}}_\mathrm{S}(\mathbf{x},\omega)$ for the wave field of the virtual source is defined as

$$\bar{\mathbf{I}}_\mathrm{S}(\mathbf{x},\omega) = \frac{1}{2} \Re\{ S(\mathbf{x},\omega) \mathbf{V}_\mathrm{S}(\mathbf{x},\omega)^* \} \;, \quad (9)$$

where $\mathbf{V}_\mathrm{S}(\mathbf{x},\omega)$ denotes the particle velocity field of the virtual source $S(\mathbf{x},\omega)$, $\Re\{\cdot\}$ the real part of its argument and the superscript $*$ the conjugate complex of a variable.

The Green's function in Eq. (7) characterizes the field of the secondary sources, the remaining terms their strength. The strength will be termed as *secondary source driving function* in the following. The secondary source driving function $D(\mathbf{x}_0,\omega)$ is given as

$$D(\mathbf{x}_0,\omega) = 2a(\mathbf{x}_0) \frac{\partial}{\partial \mathbf{n}} S(\mathbf{x}_0,\omega) \;. \quad (10)$$

The secondary source driving function plays an important role since it determines the loudspeaker signals in a practical implementation. It is the basis for three- and two-dimensional WFS approaches discussed within the scope of this paper.

Summarizing the results of this section, the sound pressure $P(\mathbf{x},\omega)$ inside the listening area can be expressed by the secondary source driving functions $D(\mathbf{x}_0,\omega)$ and the Green's functions $G(\mathbf{x}|\mathbf{x}_0,\omega)$ of the monopoles at the boundary ∂V as

$$P(\mathbf{x},\omega) = - \oint_{\partial V} D(\mathbf{x}_0,\omega)\, G_0(\mathbf{x}|\mathbf{x}_0,\omega)\, dS_0 \;. \quad (11)$$

For an arbitrarily shaped boundary ∂V the reproduced wave field will not exactly match the virtual source field $S(\mathbf{x},\omega)$ within V. However, practice has revealed that the assumptions used to derive the driving function provide a reasonable approximation for sound reproduction purposes. A detailed analysis of the resulting artifacts is an open research topic.

2.5. Virtual Source Models

Model-based rendering of a virtual sources requires appropriate models for their wave fields. This section explicitly introduces two commonly used virtual source models, plane and spherical waves. It is also shown how to determine the window function $a(\mathbf{x}_0)$ from (10) for these two special cases.

The wave field of a plane wave is given as

$$S_\mathrm{pw}(\mathbf{x},\omega) = \hat{S}_\mathrm{pw}(\omega)\, e^{-j\frac{\omega}{c}\mathbf{n}_\mathrm{pw}^T\mathbf{x}} \;, \quad (12)$$

where $\mathbf{n}_\mathrm{pw}$ denotes the propagation direction of the plane wave and $\hat{S}_\mathrm{pw}(\omega)$ its spectrum. The window function $a_\mathrm{pw}(\mathbf{x}_0)$ for a virtual plane wave can be derived by evaluating (9) for the pressure $S_\mathrm{pw}(\mathbf{x},\omega)$ and velocity field $\mathbf{V}_\mathrm{pw}(\mathbf{x},\omega)$ of a plane wave as [31]

$$a_\mathrm{pw}(\mathbf{x}_0) = \begin{cases} 1 & \text{, if } \langle \mathbf{n}_\mathrm{pw}, \mathbf{n}(\mathbf{x}_0)\rangle > 0, \\ 0 & \text{, otherwise.} \end{cases} \quad (13)$$

The wave field of a spherical wave with stationary position is given as

$$S_\mathrm{sw}(\mathbf{x},\omega) = \hat{S}_\mathrm{sw}(\omega)\, \frac{e^{-j\frac{\omega}{c}|\mathbf{x}-\mathbf{x}_S|}}{|\mathbf{x}-\mathbf{x}_S|} \;, \quad (14)$$

where $\mathbf{x}_S$ denotes the center position of the spherical wave and $\hat{S}_\mathrm{sw}(\omega)$ its spectrum in radial direction. The window function $a_\mathrm{sw}(\mathbf{x}_0)$ for a virtual spherical wave is given as [31]

$$a_\mathrm{sw}(\mathbf{x}_0) = \begin{cases} 1 & \text{, if } \langle \mathbf{x}_0 - \mathbf{x}_S, \mathbf{n}(\mathbf{x}_0)\rangle > 0, \\ 0 & \text{, otherwise.} \end{cases} \quad (15)$$

Besides these two basic types of virtual sources also other models have been developed in the past.

Models for complex sources and appropriate driving functions for WFS have been developed by e. g. [33, 34, 35, 36]. However, most of this work is based upon the assumption of a linear secondary source distribution which requires no sensible selection of the active secondary sources. Following the generalization of the linear case to curved and closed secondary source contours, given in Section 2.3, the acoustic intensity vector of the complex source can be used to select the active secondary sources in the general case.

The model of a spherical wave given by Eq. (14) is based on the assumption of a stationary source position. Most of the current implementations of WFS systems render moving sources as a sequence of stationary source positions that change over time [37]. Recently this situation has been improved by explicitly applying models of moving sources [38].

The underlying theory of WFS assumes that the listening area V is free of sources. Consequently no virtual source $S(\mathbf{x}, \omega)$ can be placed within the listening area in order to determine an appropriate driving function for that situation. However, it is possible to reproduce a point source (with some restrictions) in the listening area by applying the time-reversal principle [39, 40]. Such sources are termed as *focused sources*. Recently, the theory of focused sources has been extended to allow the reproduction of directional focused sources [41]. Note, that the proposed secondary source selection scheme (8) has to be modified to cover focused sources [31].

3. THREE-DIMENSIONAL WAVE FIELD SYNTHESIS

The generic theory of WFS developed in Section 2 holds for two- and three-dimensional WFS systems. This section will specialize the theory to the case of three-dimensional reproduction in a listening volume.

The Green's function used in the reproduction equation (11) determines the characteristics of the secondary sources. The specific form of the free-field Green's function depends on the dimensionality of the problem. The three-dimensional free-field Green's function is given as [25]

$$G_{0,3\mathrm{D}}(\mathbf{x}|\mathbf{x}_0, \omega) = \frac{1}{4\pi} \frac{e^{-j\frac{\omega}{c}|\mathbf{x}-\mathbf{x}_0|}}{|\mathbf{x}-\mathbf{x}_S|}. \qquad (16)$$

Equation (16) can be interpreted as the field of a point source with monopole characteristics located at the position $\mathbf{x}_0$.

3.1. Arbitrarily Shaped Secondary Source Contours

Three-dimensional WFS can be realized by surrounding the listening volume V by a continuous distribution of point sources placed on the boundary ∂V. These secondary sources are driven by the secondary source driving function (10). The driving function is given by the directional gradient of the virtual source wave field and the window function $a(\mathbf{x}_0)$. Hence, the explicit form of the driving function depends on the virtual source and the geometry of the sound reproduction system. The driving function for a plane wave is determined by the direction gradient of the wave field of a plane wave (12) and the window function (13) as

$$D_{\mathrm{pw},3\mathrm{D}}(\mathbf{x}_0, \omega) = \\ -2a_{\mathrm{pw}}(\mathbf{x}_0) \frac{\mathbf{n}_{\mathrm{pw}}^T \mathbf{n}(\mathbf{x}_0)}{c} j\omega \hat{S}_{\mathrm{pw}}(\omega) e^{-j\frac{\omega}{c}\mathbf{n}_{\mathrm{pw}}^T \mathbf{x}_0} . \qquad (17)$$

A time-domain version of the driving function (17) is useful to derive an efficient implementation of WFS. Inverse Fourier transformation of Eq. (17) reveals the time-domain version of the driving signal

$$d_{\mathrm{pw},3\mathrm{D}}(\mathbf{x}_0, t) = \\ -2a_{\mathrm{pw}}(\mathbf{x}_0) \frac{\mathbf{n}_{\mathrm{pw}}^T \mathbf{n}(\mathbf{x}_0)}{c} \frac{d}{dt} \hat{s}_{\mathrm{pw}}(t - \frac{\mathbf{n}_{\mathrm{pw}}^T \mathbf{x}_0}{c}) , \qquad (18)$$

where the differentiation theorem of the Fourier transformation was used. Equation (18) states that the driving signal for a plane wave can be computed efficiently in the time-domain by weighting the derivative of the time-shifted source signal $\hat{s}_{\mathrm{pw}}(t)$. However, the differentiation of the virtual source signal may also be performed by filtering the signal by a filter with $j\omega$-characteristic. This is especially useful when considering the effects of spatial aliasing (see Section 5.1).

The driving function for a virtual spherical wave can be derived by following the same procedure as outline above for a virtual plane wave. In the frequency

domain it is given as

$$D_{\mathrm{sw,3D}}(\mathbf{x}_0,\omega) = -2a_{\mathrm{sw}}(\mathbf{x}_0)\frac{(\mathbf{x}_0-\mathbf{x}_S)^T\mathbf{n}(\mathbf{x}_0)}{|\mathbf{x}_0-\mathbf{x}_S|^2}\times \\ \times\left(\frac{1}{|\mathbf{x}_0-\mathbf{x}_S|}+\frac{j\omega}{c}\right)\hat{S}_{\mathrm{sw}}(\omega)e^{-j\frac{\omega}{c}|\mathbf{x}_0-\mathbf{x}_S|}\,. \quad (19)$$

The time-domain version of the driving signal for a spherical wave is derived by inverse Fourier transformation of Eq. (19)

$$d_{\mathrm{sw,3D}}(\mathbf{x}_0,t) = -2a_{\mathrm{sw}}(\mathbf{x}_0)\frac{(\mathbf{x}_0-\mathbf{x}_S)^T\mathbf{n}(\mathbf{x}_0)}{|\mathbf{x}_0-\mathbf{x}_S|^2}\times \\ \times\left(\frac{1}{|\mathbf{x}_0-\mathbf{x}_S|}+\frac{1}{c}\frac{d}{dt}\right)\hat{s}_{\mathrm{sw}}(t-\frac{|\mathbf{x}_0-\mathbf{x}_S|}{c})\,. \quad (20)$$

For a spherical wave, the driving signal in the time-domain is given by a weighted linear superposition of the time-shifted source signal $\hat{s}_{\mathrm{sw}}(t)$ and its derivative.

Practical implementations of three-dimensional sound reproduction systems typically exhibit spherical or cuboid shape. The detailed discussion of spherical WFS systems is out of scope in this paper. A planar secondary source distribution is the basic building block of a cuboid shaped reproduction system. A planar distribution will be discussed in detail in the next section.

3.2. Planar Secondary Source Distribution

The closed contour integral (11) over the surface ∂V can be degenerated to an integral over an infinite plane. In brief, this degeneration is achieved by splitting the closed contour ∂V into a planar boundary and a half-sphere. The integration over the half-sphere can be omitted by applying the Sommerfeld radiation condition [25].

It will be assumed in the following, without loss of generality, that the secondary source distribution is located on the xz-plane at $y = 0$. Other cases can be regarded as simple translation or rotation of this special case.

The reproduced wave field for a planar distribution of secondary point sources on the xz-plane is given as

$$P(\mathbf{x},\omega) = \\ -\iint_{-\infty}^{\infty} D_{\mathrm{3D}}(\mathbf{x}_0,\omega)\,G_{0,\mathrm{3D}}(\mathbf{x}|\mathbf{x}_0,\omega)\,dx_0dz_0\,, \quad (21)$$

with $\mathbf{x}_0 = [x_0\,0\,z_0]^T$. Equation (21) is known as the first Rayleigh integral. The reproduced wave field $P(\mathbf{x},\omega)$ will be mirrored at the secondary source distribution as a consequence of the Neumann boundary condition (4). Hence, the reproduced wave field is only correct in one of the two half-volumes separated by the secondary source distribution. The direction of the normal vector $\mathbf{n}$ specifies the considered half-volume. We will consider the half-volume with $y \geq 0$ as the listening area in the sequel. The normal vector for this case is given as $\mathbf{n} = [0\,1\,0]^T$.

The secondary source driving function for a virtual plane wave is given by specializing Eq. (17). Due to the symmetry of the reproduced wave field with respect to the secondary source distribution it is reasonable to limit the incidence angle of the virtual plane wave to the case $n_{y,\mathrm{pw}} > 0$, hence to plane waves traveling into the positive y-direction. Accordingly to Eq. (13), the value of the window function for selection of active secondary sources will be $a_{\mathrm{pw}}(\mathbf{x}_0) = 1$.

The driving function for a virtual spherical wave is given by specializing Eq. (19). Due to the symmetry of the reproduced wave field with respect to the secondary source distribution it is reasonable to constrain the possible positions of the point source to $y_S < 0$. Accordingly to Eq. (15), the value of the window function for selection of active secondary sources will be $a_{\mathrm{sw}}(\mathbf{x}_0) = 1$ in this case.

Up to now, the secondary source distribution was assumed to be of infinite size and continuous. Practical implementations of three-dimensional planar WFS systems will consist of a limited number of secondary sources placed at discrete positions. Since loudspeakers will be used as secondary sources in practice, these discrete distributions of secondary sources are termed as *(planar) loudspeaker arrays*.

Two types of artifacts may emerge from the spatial truncation and discretization: (1) truncation and (2) spatial aliasing artifacts. Truncation artifacts can be analyzed by multiplying the driving function with a window modeling the aperture of the loudspeaker array, spatial sampling by multiplying the driving function with a series of spatial Dirac pulses. A detailed analysis of both artifacts is beyond the scope of this paper. However, both have been analyzed already for linear loudspeaker arrays [42]. The results derived here can be applied straightforwardly to planar loudspeakers arrays due to the separability

of the Cartesian coordinate system. A summary of aliasing, truncation and other artifacts of WFS can be found in Section 5.

The reproduced wave field for a planar continuous distribution of infinite size will exactly match the wave field of the virtual source within the listening area. This can be proven by inserting the driving functions into the reproduction equation (21). Artifacts will occur for other geometries of the secondary source distribution. This is due to the fact that the derived Neumann Green's function only fulfills the required Neumann boundary condition exactly in this special case.

3.3. Example for Planar Secondary Source Distribution

Figure 2 illustrates the wave field reproduced by a planar loudspeaker array in the plane $z = 0$. The loudspeaker array consist of 100×100 point sources with a distance of $\Delta x = \Delta y = 0.15$ m between them. The rather high number of loudspeakers has been chosen to avoid significant aperture and aliasing artifacts in the illustrated region. Figure 2(a) shows the reproduced wave field when using the plane wave driving function (17) for the reproduction of a monochromatic virtual plane wave with frequency $f_{\mathrm{pw}} = 500$ Hz and propagation direction $\mathbf{n}_{\mathrm{pw}} = [0\,1\,0]^T$. Accordingly to [42] spatial aliasing will only occur for frequencies above 2 kHz for this configuration.

Figure 2(b) shows the reproduced wave field when using the spherical wave driving function (19) for the reproduction of a monochromatic virtual spherical wave with frequency $f_{\mathrm{sw}} = 500$ Hz and position $\mathbf{x}_S = [0\ -2\ 0]^T$ m. It can be seen clearly that both wave fields are reproduced accurately by the planar distribution of secondary point sources.

4. TWO-DIMENSIONAL WAVE FIELD SYNTHESIS

The technical realization of a three-dimensional WFS system would involve a very high number of loudspeakers and reproduction channels. The majority of WFS systems realized so far are therefore restricted to the reproduction in a plane only. This reduction of dimensionality is reasonable for most scenarios due to the spatial characteristics of human hearing. Preferably this listening plane should be leveled with the listeners ears. Such systems will be termed as *two-dimensional WFS* systems in the following. The reduction in dimensionality has one major drawback: two-dimensional WFS systems are not capable to reproduce wave fields which have contributions emerging from sources above or below the plane where the loudspeakers are contained in. However, this restriction holds also for most of the currently applied surround systems. Note, that in the following all position vectors are assumed to be two-dimensional.

4.1. Line Sources as Secondary Sources

The generic theory of WFS developed in Section 2 can be specialized to two-dimensional reproduction by using the two-dimensional free-field Green's function as wave field for the secondary sources. The two-dimensional free-field Green's function is given as [25]

$$G_{2\mathrm{D}}(\mathbf{x}|\mathbf{x}_0,\omega) = \frac{j}{4} H_0^{(2)}(\frac{\omega}{c}\,|\mathbf{x}-\mathbf{x}_0|)\ , \qquad (22)$$

where $H_0^{(2)}(\cdot)$ denotes the zeroth-th order Hankel function of second kind [43]. For the definition of a two-dimensional wave field used within the context of this paper, Eq. (22) can be interpreted as the field of a line source. This line source is located parallel to the z-axis and intersects with the reproduction plane at the position $\mathbf{x}_0$.

Loudspeakers that approximately have the properties of line sources are hardly available. For instance such a loudspeaker should have infinite length which is not realizable. Hence, using line sources as secondary sources for WFS serves more as theoretical framework to derive various properties of WFS and for illustration purposes. Therefore, this scenario is only discussed in brief here.

Note, that in a truly two-dimensional wave propagation scenario, Eq. (22) represents the wave field produced by a spatio-temporal Dirac pulse at the position $\mathbf{x}_0$.

The driving function for virtual plane wave, as derived in Section 3.1, is independent from the underlying dimensionality of the wave fields. Hence, Eq. (17) holds also for two-dimensional WFS (with $n_{z,\mathrm{pw}} = 0$) using line sources as secondary sources. The driving function for a virtual plane wave can be derived straightforwardly from Eq. (17) by using the two-dimensional normal vector $\mathbf{n}_{\mathrm{pw}} = [\cos\theta_{\mathrm{pw}}\ \ \sin\theta_{\mathrm{pw}}]^T$ where θ_{pw} denotes the incidence angle of the plane wave.

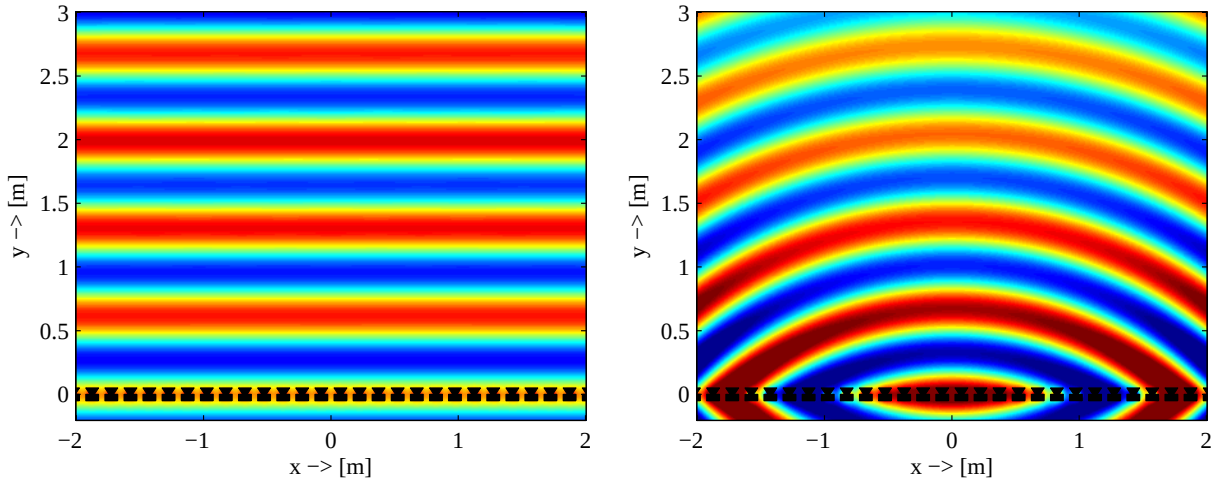

(a) plane wave ($f_{\mathrm{pw}} = 500$ Hz, $\mathbf{n}_{\mathrm{pw}} = [0\,1\,0]^T$)

(b) spherical wave ($f_{\mathrm{sw}} = 500$ Hz, $\mathbf{x}_S = [0\ -2\ 0]^T$ m)

Fig. 2: Wave fields reproduced in the plane $z = 0$ by a planar secondary source distribution of 100×100 point sources with a distance of $\Delta x = \Delta y = 0.15$ m between them.

In two-dimensional wave propagation the wave field of a line source is given by Eq. (22). The corresponding virtual wave field will be termed as virtual *cylindrical wave* in the following. The driving function for a virtual cylindrical wave placed at the position $\mathbf{x}_S$ can be derived as

$$D_{\mathrm{cy,2D}}(\mathbf{x}_0, \omega) = -\frac{1}{2c} a_{\mathrm{cy}}(\mathbf{x}_0) \frac{(\mathbf{x}_0 - \mathbf{x}_S)^T \mathbf{n}(\mathbf{x}_0)}{|\mathbf{x}_0 - \mathbf{x}_S|} \times \\ \times \frac{j\omega}{c} \hat{S}_{\mathrm{cy}}(\omega) H_1^{(2)}(\frac{\omega}{c} |\mathbf{x}_0 - \mathbf{x}_S|) \,, \quad (23)$$

where $a_{\mathrm{cy}} = a_{\mathrm{sw}}$ due to the radial symmetry of both line sources and point sources.

Figure 3 illustrates the wave field reproduced by a linear distribution of line sources. The loudspeaker array consists of 100 line sources with a distance of $\Delta x = 0.15$ m between them. Figure 3(a) shows the reproduced wave field when using the plane wave driving function (17), Fig. 3(b) shows the reproduced wave field when using the cylindrical wave driving function (23). It can be seen clearly that both wave fields are reproduced accurately by the linear distribution of secondary line sources.

Please note, that using the driving function (19) of a spherical wave for two-dimensional WFS will result in artifacts in the reproduced wave field, most notably an incorrect amplitude decay.

4.2. Point Sources as Secondary Sources

It has been shown in the previous section that line sources are the appropriate choice as secondary sources for two-dimensional WFS. However, it is desirable to use loudspeakers with closed cabinets as secondary sources, due to the fact that such loudspeakers are widely available. These approximately have the characteristics of an acoustic point source. In order to analyze and compensate the error introduced by this secondary source type mismatch a closer look is taken at the properties of point and line sources. The asymptotic expansion of the Hankel functions for large arguments [43] is used to approximate the two-dimensional Green's function $G_{\mathrm{2D}}(\mathbf{x}|\mathbf{x}_0, \omega)$ as follows

$$G_{\mathrm{2D}}(\mathbf{x}|\mathbf{x}_0, \omega) \approx \sqrt{\frac{2\pi\,|\mathbf{x} - \mathbf{x}_0|}{j\frac{\omega}{c}}} \underbrace{\frac{1}{4\pi} \frac{e^{-j\frac{\omega}{c}|\mathbf{x}-\mathbf{x}_0|}}{|\mathbf{x} - \mathbf{x}_0|}}_{G_{\mathrm{3D}}(\mathbf{x}|\mathbf{x}_0,\omega)} \,. \quad (24)$$

Comparing the right fraction of Eq. (24) with Eq. (16) reveals that the given approximation of $G_{\mathrm{2D}}(\mathbf{x}|\mathbf{x}_0, \omega)$ is equivalent to $G_{\mathrm{3D}}(\mathbf{x}|\mathbf{x}_0, \omega)$ when applying a spectral and amplitude correction. Note that the corrections outlined above assume that the large argument approximation ($\frac{\omega}{c} |\mathbf{x} - \mathbf{x}_0| \gg 1$) holds. For low frequencies and positions close to the

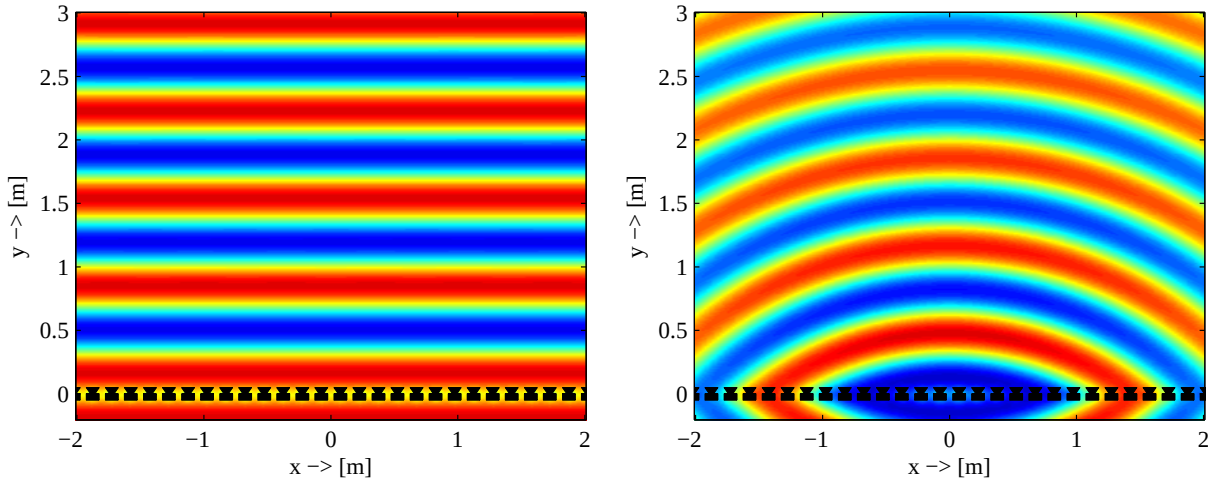

(a) plane wave ($f_{\mathrm{pw}} = 500$ Hz, $\mathbf{n}_{\mathrm{pw}} = [0\,1]^T$)

(b) cylindrical wave ($f_{\mathrm{cy}} = 500$ Hz, $\mathbf{x}_S = [0\ -2]^T$ m)

Fig. 3: Wave fields reproduced by a linear distribution of 100 secondary line sources with a distance of $\Delta x = 0.15$ m between them.

secondary sources this approximation might be inaccurate. The large argument approximation of the Hankel function is also known as far-field or stationary phase approximation.

Introducing the approximation (24) of the two-dimensional free-field Green's function into Eq. (11) yields

$$P(\mathbf{x},\omega) = -\oint_{\partial V} \sqrt{\frac{2\pi\,|\mathbf{x}-\mathbf{x}_0|}{j\frac{\omega}{c}}}\, D_{2\mathrm{D}}(\mathbf{x}_0,\omega)\, G_{3\mathrm{D}}(\mathbf{x}|\mathbf{x}_0,\omega)\, dS_0\ . \tag{25}$$

The compensation of the secondary source type mismatch can be included into the driving function used for two-dimensional WFS with point sources as secondary sources. It can be seen from Eq. (25) that the required spectral correction is independent from the receiver position $\mathbf{x}$. However, the amplitude correction depends on the receiver position. As a consequence, the amplitude can only be corrected for one receiver position in the listening area. For other positions, amplitude errors will be present. The position that is used for the amplitude correction is denoted by $\mathbf{x}_{\mathrm{ref}}$ in the following.

The corrected driving function is then given as

$$D_{2.5\mathrm{D}}(\mathbf{x}_0,\omega) = \sqrt{\frac{1}{j\frac{\omega}{c}}}\ \sqrt{2\pi\,|\mathbf{x}_{\mathrm{ref}}-\mathbf{x}_0|}\ D_{2\mathrm{D}}(\mathbf{x}_0,\omega)\ , \tag{26}$$

where the notation 2.5D accounts for the mixture of two dimensional reproduction using point sources as secondary sources.

The driving function for a virtual plane wave can be derived straightforwardly by introducing Eq. (17) into Eq. (26) as

$$D_{\mathrm{pw},2.5\mathrm{D}}(\mathbf{x}_0,\omega) = -2a_{\mathrm{pw}}(\mathbf{x}_0)\sqrt{2\pi\,|\mathbf{x}_{\mathrm{ref}}-\mathbf{x}_0|}\times \times \sqrt{j\frac{\omega}{c}}\hat{S}_{\mathrm{pw}}(\omega)\mathbf{n}_{\mathrm{pw}}^T\mathbf{n}(\mathbf{x}_0)e^{-j\frac{\omega}{c}\mathbf{n}_{\mathrm{pw}}^T\mathbf{x}_0}\ . \tag{27}$$

Inverse Fourier transformation of Eq. (27) reveals the time-domain driving function

$$d_{\mathrm{pw},2.5\mathrm{D}}(\mathbf{x}_0,t) = w_{\mathrm{pw}}\ \delta(t-\frac{\mathbf{n}_{\mathrm{pw}}^T\mathbf{x}_0}{c}) * (f_{\mathrm{pw}}(t) * \hat{s}_{\mathrm{pw}}(t))\ , \tag{28}$$

where all weighting terms have been combined into $w_{\mathrm{pw}} = -2a_{\mathrm{pw}}(\mathbf{x}_0)\sqrt{2\pi\,|\mathbf{x}_{\mathrm{ref}}-\mathbf{x}_0|}\mathbf{n}_{\mathrm{pw}}^T\mathbf{n}(\mathbf{x}_0)$ and $f_{\mathrm{pw}}(t)$ is given by the inverse Fourier transformation of $\sqrt{j\frac{\omega}{c}}$. Equation (28) states that the driving signal

for a virtual plane wave can be computed efficiently in the time-domain by weighting and delaying the pre-filtered source signal $\hat{s}_{\mathrm{pw}}(t)$. Note, that the pre-filtering is independent from the secondary source position. Hence, it only has to be performed once for all secondary sources in advance to the secondary source dependent weighting and delaying. It is interesting to note that the pre-filtering by $f_{\mathrm{pw}}(t)$ can also be understood as taking the half-derivative of the source signal $\hat{s}_{\mathrm{pw}}(t)$.

The driving function for a cylindrical wave was derived in Section 4.1. Since, we are aiming at two-dimensional WFS this would be the appropriate driving function at first sight. However, line sources don't exhibit a flat frequency response as can be seen from (22). In oder to overcome this drawback, point source models are typically used as virtual source model in two-dimensional WFS with point sources as secondary sources.

The driving function for a virtual spherical wave is given by introducing the driving function for a spherical wave (19) into Eq. (26)

$$\begin{aligned} &D_{\mathrm{sw,2.5D}}(\mathbf{x}_0,\omega) = \\ &-2a_{\mathrm{sw}}(\mathbf{x}_0)\frac{(\mathbf{x}_0-\mathbf{x}_S)^T\mathbf{n}(\mathbf{x}_0)}{|\mathbf{x}_0-\mathbf{x}_S|}\sqrt{2\pi\,|\mathbf{x}_{\mathrm{ref}}-\mathbf{x}_0|}\times \\ &\times\left(\frac{1}{\sqrt{j\frac{\omega}{c}}\,|\mathbf{x}_0-\mathbf{x}_S|}+\sqrt{\frac{j\omega}{c}}\right)\hat{S}_{\mathrm{sw}}(\omega)\frac{e^{-j\frac{\omega}{c}|\mathbf{x}_0-\mathbf{x}_S|}}{|\mathbf{x}_0-\mathbf{x}_S|}\ . \end{aligned} \tag{29}$$

The time-domain driving function, derived by inverse Fourier transformation of Eq. (29), reads

$$\begin{aligned} &d_{\mathrm{sw,2.5D}}(\mathbf{x}_0,t) = \\ &\quad w_{\mathrm{sw}}\ \delta(t-\frac{|\mathbf{x}_0-\mathbf{x}_S|}{c}) * (f_{\mathrm{sw}}(t) * \hat{s}_{\mathrm{sw}}(t))\ , \end{aligned} \tag{30}$$

where all weighting factors have been collected in w_{sw}. The pre-filter $f_{\mathrm{sw}}(t)$ is defined as follows

$$f_{\mathrm{sw}}(t) = \mathcal{F}^{-1}\left\{\left(\frac{1}{\sqrt{j\frac{\omega}{c}}\,|\mathbf{x}_0-\mathbf{x}_S|}+\sqrt{\frac{j\omega}{c}}\right)\right\}\ , \tag{31}$$

where $\mathcal{F}^{-1}$ denotes the inverse Fourier transformation. As for the plane wave, the driving signal for a spherical wave can be computed efficiently in the time domain by weighting and delaying the pre-filtered source signal.

Figure 4 illustrates the wave field reproduced by a circular distribution of point sources. The loudspeaker array consist of 56 equiangular positioned point sources with a radius of $R = 1.50$ m. Figure 4(a) shows the reproduced wave field when using the plane wave driving function (27), Fig. 4(b) shows the reproduced wave field when using the spherical wave driving function (29). The secondary source selection criterion is indicated by the solid loudspeaker symbols. The amplitude errors inherent to the use of secondary point sources for two-dimensional reproduction can be seen clearly in Fig. 4(a). A plane wave is supposed not to lose amplitude over distance.

4.3. Linear Distributions of Secondary Point Sources

The wave field reproduced by a linear distribution of secondary point sources is given by specializing Eq. (25) to a linear geometry

$$P(\mathbf{x},\omega) = -\int_{-\infty}^{\infty} D_{\mathrm{2.5D}}(\mathbf{x}_0,\omega)\,G_{\mathrm{3D}}(\mathbf{x}|\mathbf{x}_0,\omega)\,dx_0\ , \tag{32}$$

where it is assumed that the secondary source distribution is located on the x-axis. The integral (32) is also known as the 2.5-dimensional Rayleigh integral [6, 5].

It was shown in [29] that a linear distribution of secondary point sources is capable of reproducing the amplitude correctly only on a line parallel to the secondary source distribution. This was also shown in the traditional WFS literature within the limitations of the stationary phase approximation. Hence, the amplitude correction by $\sqrt{2\pi\,|\mathbf{x}_{\mathrm{ref}}-\mathbf{x}_0|}$ in Eq. (26) can be assumed to be constant for the linear case.

The driving functions for plane and spherical waves that have been derived in the previous section can be applied straightforwardly to the linear case. The reproduced wave field will be symmetrical to the x-axis. Hence, the incidence angle of the virtual plane wave has to be restricted to $n_{y,\mathrm{pw}} > 0$ and the position of the virtual point source to $y_S < 0$. As for the planar secondary source distribution discussed in Section 3.2 no explicit secondary source selection is required in this case.

Figure 5 illustrates the wave field reproduced by a linear distribution of secondary point sources for a virtual plane wave and spherical wave. The

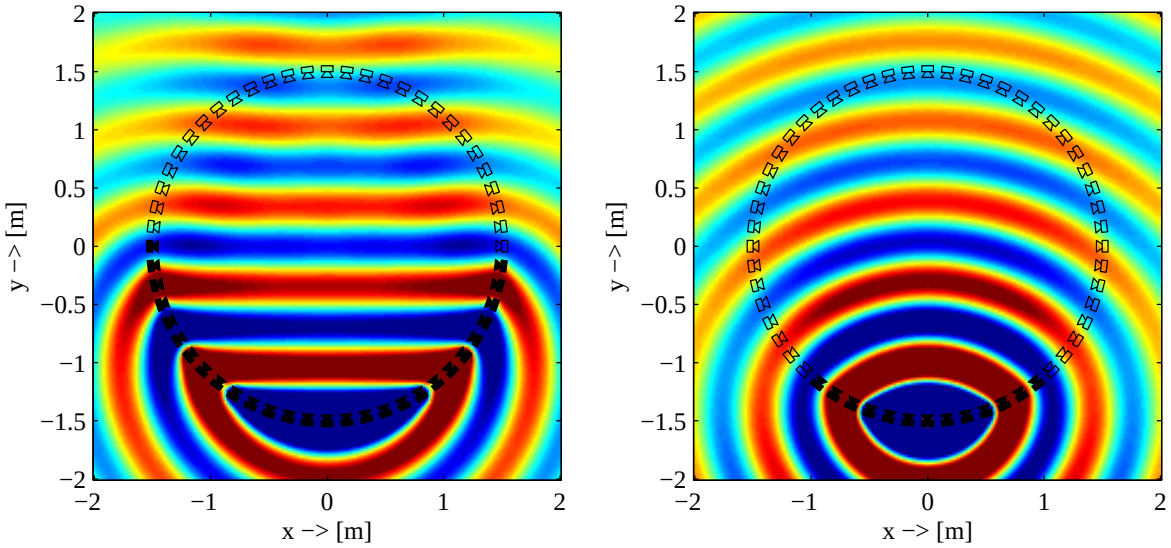

(a) plane wave ($f_{\mathrm{pw}} = 500$ Hz, $\mathbf{n}_{\mathrm{pw}} = [0\,1]^T$)

(b) spherical wave ($f_{\mathrm{sw}} = 500$ Hz, $\mathbf{x}_S = [0\ -2]^T$ m)

Fig. 4: Wave fields reproduced by a circular distribution of 56 point sources with a radius of $R = 1.50$ m. The active secondary sources are indicated by the solid loudspeaker symbols.

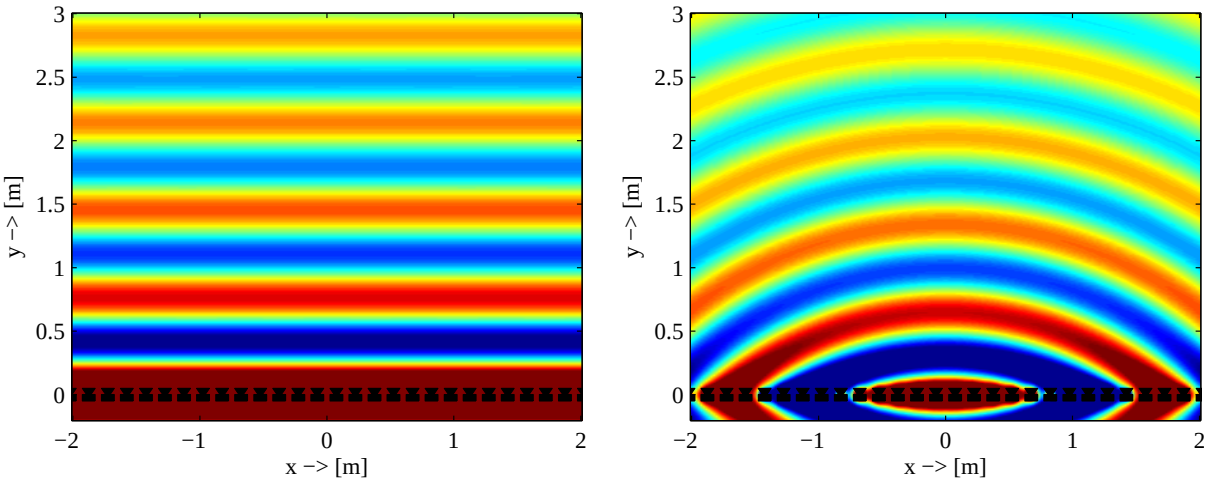

(a) plane wave ($f_{\mathrm{pw}} = 500$ Hz, $\mathbf{n}_{\mathrm{pw}} = [0\,1]^T$)

(b) spherical wave ($f_{\mathrm{sw}} = 500$ Hz, $\mathbf{x}_S = [0\ -2]^T$ m)

Fig. 5: Wave fields reproduced by a linear distribution of 100 secondary point sources with a distance of $\Delta x = 0.15$ m between them.

wave field for a virtual plane wave is shown in Fig. 5(a), the wave field for a virtual spherical wave in Fig. 5(b). The amplitude errors inherent to the use of secondary point sources in this situation can be seen clearly in Fig. 5(a).

4.4. Comparison to the Traditional Formulation of WFS

In this section, we provide a link between the traditional WFS formulation [6] and the proposed one. As denoted in Section 2.3, the traditional WFS literature has concentrated on linear distributions of secondary point sources reproducing a monopole point source. We will therefore exemplarily consider this special case.

The traditional WFS formulation of the driving function $D_{\mathrm{trad}}(\mathbf{x}_0,\omega)$ for a linear distribution of secondary point sources parallel to the x-axis at $y=y_0$ reproducing a monopole point source at position $\mathbf{x}_\mathrm{S}$ reads [6]

$$D_{\mathrm{trad}}(\mathbf{x}_0,\omega) = \hat{S}(\omega)\sqrt{\frac{j\frac{\omega}{c}}{2\pi}}\times \\ \times\sqrt{\frac{|\mathbf{x}_\mathrm{ref}-\mathbf{x}_0|}{|\mathbf{x}_\mathrm{S}-\mathbf{x}_0|+|\mathbf{x}_\mathrm{ref}-\mathbf{x}_0|}}\;\cos\phi\;\frac{e^{-j\frac{\omega}{c}|\mathbf{x}_\mathrm{S}-\mathbf{x}_0|}}{\sqrt{|\mathbf{x}_\mathrm{S}-\mathbf{x}_0|}}\,, \tag{33}$$

whereby ϕ denotes the angle between the y-axis and the vector $\mathbf{x}_\mathrm{S}-\mathbf{x}_0$. With

$$\cos\phi = \frac{-y_\mathrm{S}}{|\mathbf{x}_\mathrm{S}-\mathbf{x}_0|} \tag{34}$$

equation (33) becomes

$$D_{\mathrm{trad}}(\mathbf{x}_0,\omega) = \hat{S}(\omega)\sqrt{\frac{j\frac{\omega}{c}}{2\pi}}\times \\ \times\sqrt{\frac{|\mathbf{x}_\mathrm{S}-\mathbf{x}_0|\cdot|\mathbf{x}_\mathrm{ref}-\mathbf{x}_0|}{|\mathbf{x}_\mathrm{S}-\mathbf{x}_0|+|\mathbf{x}_\mathrm{ref}-\mathbf{x}_0|}}\;\frac{-y_\mathrm{S}}{|\mathbf{x}_\mathrm{S}-\mathbf{x}_0|}\;\frac{e^{-j\frac{\omega}{c}|\mathbf{x}_\mathrm{S}-\mathbf{x}_0|}}{|\mathbf{x}_\mathrm{S}-\mathbf{x}_0|}\,. \tag{35}$$

For $|\mathbf{x}_\mathrm{S}-\mathbf{x}_0| \gg 1$, thus when the virtual source is positioned far behind the secondary sources, (35) simplifies to

$$D_{\mathrm{trad}}(\mathbf{x}_0,\omega) \approx \hat{S}(\omega)\sqrt{\frac{j\frac{\omega}{c}}{2\pi}}\times \\ \times\sqrt{|\mathbf{x}_\mathrm{ref}-\mathbf{x}_0|}\;\frac{-y_\mathrm{S}}{|\mathbf{x}_\mathrm{S}-\mathbf{x}_0|}\;\frac{e^{-j\frac{\omega}{c}|\mathbf{x}_\mathrm{S}-\mathbf{x}_0|}}{|\mathbf{x}_\mathrm{S}-\mathbf{x}_0|}\,. \tag{36}$$

The proposed driving function $D_{\mathrm{sw,2.5D}}(\mathbf{x}_0,\omega)$ for a linear secondary source distribution reproducing a monopole point source at position $\mathbf{x}_\mathrm{S}$ including 2.5D correction can be found in equation (29). In the following we assume that the secondary source distribution is positioned parallel to the x-axis at $y=y_0$. For $|\mathbf{x}_\mathrm{S}-\mathbf{x}_0| \gg 1$ the addend $1/\sqrt{\frac{\omega}{c}|\mathbf{x}_\mathrm{S}-\mathbf{x}_0|}$ in (29) becomes insignificant compared to the added $\sqrt{j\omega}/c$ and (29) then reads

$$D_{\mathrm{sw,2.5D}}(\mathbf{x}_0,\omega) \approx \hat{S}(\omega)\sqrt{2\pi j\frac{\omega}{c}}\times \\ \times\sqrt{|\mathbf{x}_\mathrm{ref}-\mathbf{x}_0|}\frac{-y_\mathrm{S}}{|\mathbf{x}_\mathrm{S}-\mathbf{x}_0|}\;\frac{e^{-j\frac{\omega}{c}|\mathbf{x}_\mathrm{S}-\mathbf{x}_0|}}{|\mathbf{x}_\mathrm{S}-\mathbf{x}_0|}\,. \tag{37}$$

Equation (36) and (37) are similar except for a normalization factor. Thus, when the virtual sound source is sufficiently far behind the secondary source distribution ($|\mathbf{x}_\mathrm{S}-\mathbf{x}_0| \gg 1$), the two driving functions are equal.

5. ARTIFACTS OF WFS

The following section will briefly discuss various artifacts that emerge from practical aspects and the assumptions made to derive the driving functions. Note that most of these artifacts may also be present in other sound field reproduction techniques, like for instance higher-order Ambisonics.

5.1. Spatial Sampling of Secondary Source Distribution

The theory presented so far assumes a spatially continuous distribution of secondary sources. Practical implementations of WFS will consist of secondary sources that are placed at spatially discrete positions. This spatial sampling of the continuous distribution may lead to spatial aliasing artifacts in the reproduced wave field. Spatial aliasing constitutes a disturbance of the spatial structure of the reproduced wave field. Therefore, it potentially may result in localization inaccuracies and coloration artifacts.

The effects of spatial sampling on the reproduced wave field have been evaluated in the literature on WFS [42, 44, 12, 45]. An analysis of aliasing artifacts is only possible when considering a particular geometry of the secondary source distribution contour. However, two main conclusions can be drawn: (1) spatial aliasing increases with the bandwidth

of the virtual source signal and (2) spatial aliasing artifacts depend on the listener position. Typical WFS systems employ loudspeakers with a spacing of $\Delta x = 10...30$ cm. The resulting spatial aliasing artifacts become prominent for frequencies of the virtual source of roughly above 1 kHz (spatial aliasing frequency). This would indicate that WFS cannot be used for the auralization of typical audio sources. However, the human auditory system seems to be not too sensible to spatial aliasing if the loudspeaker spacing is chosen in the range $\Delta x = 10...30$ cm. A detailed analysis of the perceptual impact of spatial aliasing is an current research topic. The results in [11] indicate that spatial aliasing may lead to coloration.

The various WFS driving functions derived in this paper contain a pre-filtering of the virtual source signal with $j\frac{\omega}{c}$ or $\sqrt{j\frac{\omega}{c}}$ characteristic, respectively. The pre-filtering of the virtual source signal should only be performed below the spatial aliasing frequency, since the theoretical foundation for the pre-filtering holds only there. A flat response above the spatial aliasing frequency has proven to be suitable in practice. Since the spatial aliasing frequency is different for different listener positions this may lead to additional coloration artifacts for listener positions the filter hasn't been optimized for.

5.2. Truncation of Secondary Source Distribution

Practical implementations of secondary source distributions with non-closed contours will always be of finite size. The theory of WFS assumes closed contours, infinitely long linear or infinitely sized planar distributions. The truncation of the secondary source distribution leads to artifacts. These artifacts in the reproduced wave field are referred to as truncation artifacts in the context of WFS.

The effects emerging from the truncation of linear secondary source contours used for WFS have been investigated in detail by [7, 6, 46]. The effect of truncating the length of a linear secondary source distribution can be qualitatively understood as the effect a gap has on a propagating wave field. Two effects can be observed [46]: (1) the area of the correctly reproduced wave field is limited by the finite aperture and (2) circular waves propagate from the outer secondary sources. The first effect can be described by ray theory, the latter by diffraction theory. Note, that due to the separability of the Cartesian coordinate systems these considerations also hold for planar secondary source distributions.

It has been shown that truncation artifacts can be reduced by applying a weight (tapering window) to the secondary source driving signals. Typically a one-sided squared cosine window is applied to the loudspeaker driving signals in order to reduce the artifacts. As a side effect, tapering will reduce the effective listening area.

Depending on the desired virtual source field, the secondary source selection criterion (8) may limit the number of active loudspeakers. This constitutes essentially a truncation of the secondary source contour and may lead to truncation artifacts. It was proposed in [31] to apply a tapering window to the driving signals which depends on the active secondary sources and the actual virtual source to be reproduced.

5.3. Amplitude Errors

Two-dimensional WFS systems typically use point sources (or their approximations by loudspeakers) as secondary sources. As already outlined in Section 4.2, this secondary source type mismatch leads to amplitude errors in the reproduced wave field. An detailed analysis of these amplitude errors can be found in [47, 16]. For the reproduction of virtual plane waves, these amplitude errors have the consequence that the reproduced wave field will exhibit an amplitude decay within the listening area. The resulting amplitude decay is approximately 3 dB per doubling of distance. The reproduced wave field for a virtual spherical wave will exhibit an amplitude decay which is inbetween the amplitude decay of a cylindrical wave and a spherical wave.

5.4. Other Artifacts

Two other artifacts of WFS are discussed briefly in the following. The first artifact is related to the reproduction of moving virtual sources, the other to the reproduction in a plane only.

Moving virtual point sources are typically reproduced by using the model of a stationary spherical wave and changing its position over time. This leads to various artifacts as reported in [37, 38]. It was proposed in this context to use the model of a moving point source to derive the secondary source driving function. This way some of these artifacts are resolved. However, the results presented in [38],

using such a model, indicate that spatial aliasing and truncation artifacts play a more prominent role in the auralization of moving virtual sources than for stationary sources.
The reproduction in a plane only (two-dimensional WFS) using point sources as secondary sources will lead to artifacts for listeners which are not located in the plane where the loudspeakers are. Its not always possible to level the loudspeakers with the listeners ears due to technical restrictions. As a consequence out of plane listeners will have the impression that the virtual sources are elevated or lowered.

6. EXTENSIONS TO WFS

So far, the basic theory of WFS and some of its artifacts have been discussed. However, WFS has been improved in various directions to cope with the problem of spatial aliasing, the listening room acoustics, the properties of real loudspeakers and noise sources. These extensions are briefly reviewed.

6.1. Enhancement of Spatial Aliasing

The relatively low spatial aliasing frequency of typical WFS systems implies potential problems in terms of coloration and localization of virtual sources. Various techniques have been proposed to enhance the situation.
It is proposed in [48, 11] to combine WFS with stereophonic techniques in order to improve coloration artifacts that arise from spatial aliasing. This technique has been termed as *optimized phantom source imaging (OPSI)*. The WFS driving functions are used below the spatial aliasing frequency, while above the spatial aliasing frequency amplitude panning with selected loudspeakers is used. The results reported so far show that OPSI provides the potential to reduce coloration artifacts while preserving most of the good localization properties of WFS.
Another technique proposed to improve the perception of spatial aliasing artifacts is to randomize the phase above the spatial aliasing frequency in the driving function [5]. The basic idea of this approach is to smear out the spatial structure of spatial aliasing. The results reported in [49] using diffuse filters show some potential.

6.2. Active Listening Room and Loudspeaker Compensation

The basic theory of WFS, as presented in Section 2, relies on free-field wave propagation and does not consider the influence of reflections within the listening environment. Since these reflections may impair the carefully designed spatial sound field, their influence should be minimized by taking appropriate countermeasures. Besides passively damping of the listening room various active techniques have been proposed e. g. [50, 51, 52, 53, 54, 55, 47, 10, 56, 57, 58, 59, 60, 61]. Common to all of these approaches is that they perform a pre-filtering of the loudspeaker driving signals in order to cancel the listening room reflections by destructive interference. However, suitable control is only achievable when no spatial aliasing is present in the reproduced wave field. Due to the varying characteristics of the propagation medium and the acoustic environment an adaptive computation of these pre-filters on basis of the reproduced wave field is desirable. Simulation results indicate that active listening room compensation provides the potential to reduce the effects of the listening room.
Besides the influence of the listening room, also non-ideal characteristics of the secondary sources may degrade the reproduced wave field. The compensation of non-ideal secondary source characteristics is known as *loudspeaker compensation* in the context of WFS. Loudspeaker compensation can be seen as subset of listening room compensation. However, no adaptive filters are required in this case since the characteristics of the loudspeakers can be assumed to be constant over time. Multichannel techniques have been proposed to perform loudspeaker compensation [62, 12].

6.3. Active Noise Control

Another kind of impairments are noise sources within the listening room. If these sources are located outside the listening area, active noise control (ANC) techniques can be applied. The signal processing techniques used for ANC are similar to those used for active listening room compensation. Hence, the same algorithms can be applied in principle to ANC for WFS. First results can be found in [63, 64, 65, 66]

7. CONCLUSION

This paper presents a generalized theory for WFS. Three-dimensional reproduction in a listening volume, as well as two-dimensional reproduction in a listening area is covered. In the latter case, both the

reproduction using secondary line and point sources has been considered. It has been shown that an exact reproduction of a desired virtual wave field is only possible with a planar continuous distribution of secondary point sources or a linear continuous distribution of secondary line sources. All other cases are approximations that may lead to artifacts in the reproduced wave field. The paper also discusses various artifacts of WFS. The most prominent ones are spatial aliasing and amplitude artifacts. Both degrade the perceived quality.

8. REFERENCES

[1] W.B. Snow. Basic principles of stereophonic sound. *IRE Transactions on Audio*, 3:42–53, March 1955.

[2] A.J. Berkhout. A holographic approach to acoustic control. *Journal of the Audio Engineering Society*, 36:977–995, December 1988.

[3] A.J. Berkhout, D. de Vries, and P. Vogel. Acoustic control by wave field synthesis. *Journal of the Acoustic Society of America*, 93(5):2764–2778, May 1993.

[4] S. Brix, T. Sporer, and J. Plogsties. CARROUSO - An European approach to 3D-audio. In *110th AES Convention*. Audio Engineering Society (AES), May 2001.

[5] E.W. Start. *Direct Sound Enhancement by Wave Field Synthesis*. PhD thesis, Delft University of Technology, 1997.

[6] E.N.G. Verheijen. *Sound Reproduction by Wave Field Synthesis*. PhD thesis, Delft University of Technology, 1997.

[7] P. Vogel. *Application of Wave Field Synthesis in Room Acoustics*. PhD thesis, Delft University of Technology, 1993.

[8] W. de Bruijn. *Application of Wave Field Synthesis in Videoconferencing*. PhD thesis, Delft University of Technology, 2004.

[9] E. Hulsebos. *Auralization using Wave Field Synthesis*. PhD thesis, Delft University of Technology, 2004.

[10] S. Spors. *Active Listening Room Compensation for Spatial Sound Reproduction Systems*. PhD thesis, University of Erlangen-Nuremberg, 2006.

[11] H. Wittek. *Perceptual differences between wavefield synthesis and stereophony*. PhD thesis, University of Surrey, 2007.

[12] E. Corteel. *Caractérisation et Extensions de la Wave Field Synthesis en conditions réelles d'écoute*. PhD thesis, Université de Paris VI, 2006.

[13] M.A.J. Baalman. *On Wave Field Synthesis and electro-acoustic music, with particular focus on the reproduction of arbitrarily shaped sound sources*. PhD thesis, Technische Universität Berlin, 2008.

[14] R. Nicol. *Restitution sonore spatialisé sur une zone étendue: Application à la téléprésence*. PhD thesis, Université du Maine, 1999.

[15] D. de Vries, E.W. Start, and V.G. Valstar. The Wave Field Synthesis concept applied to sound reinforcement: Restrictions and solutions. In *96th AES Convention*, Amsterdam, Netherlands, February 1994. Audio Engineering Society (AES).

[16] J.-J. Sonke, D. de Vries, and J. Labeeuw. Variable acoustics by wave field synthesis: A closer look at amplitude effects. In *104th AES Convention*, Amsterdam, Netherlands, May 1998. Audio Engineering Society (AES).

[17] G. Theile, H. Wittek, and M. Reisinger. Potential wavefield synthesis applications in the multichannel stereophonic world. In *AES 24th International Conference on Multichannel Audio*, Banff, Canada, June 2003. Audio Engineering Society (AES).

[18] B. Pueo, J. Escolano, S. Bleda, and J.J. Lopez. An approach for wave field synthesis high power applications. In *118th AES Convention*, Barcelona, Spain, May 2005. Audio Engineering Society (AES).

[19] T. Sporer. Wave field synthesis – Generation and reproduction of natural sound environments. In *7th International Conference on*

Digital Audio Effects (DAFx-04), Naples, Italy, Oct. 2004.

[20] A. Wagner, A. Walther, , F. Melchior, and M. Strauß. Generation of highly immersive atmospheres for wave field synthesis reproduction. In *116th AES Convention*, Berlin, Germany, 2004. Audio Engineering Society (AES).

[21] H. Wittek, S. Kerber, F. Rumsey, and G. Theile. Spatial perception in wave field synthesis rendered sound fields: Distance of real and virtual nearby sources. In *116th AES Convention*, Berlin, Germany, 2004. Audio Engineering Society (AES).

[22] S. Spors, H. Teutsch, and R. Rabenstein. High-quality acoustic rendering with wave field synthesis. *In Vision, Modelling and Visualization (VMV)*, pages 101–108, November 2001.

[23] R. Rabenstein and S. Spors. Wave field synthesis techniques for spatial sound reproduction. In E. Haensler and G. Schmidt, editors, *Topics in Acoustic Echo and Noise Control*, chapter 13, pages 517–545. Springer, 2006.

[24] R. Rabenstein and S. Spors. Sound field reproduction. In J. Benesty, M. Sondhi, and Y. Huang, editors, *Springer Handbook on Speech Processing*, chapter 53. Springer, 2007.

[25] E.G. Williams. *Fourier Acoustics: Sound Radiation and Nearfield Acoustical Holography*. Academic Press, 1999.

[26] J. Daniel. *Représentation de champs acoustiques, application à la transmission et à la reproduction de scènes sonores complexes dans un contexte multimédia*. PhD thesis, Université Paris 6, 2000.

[27] M.A. Gerzon. With-heigth sound reproduction. *Journal of the Audio Engineering Society (JAES)*, 21:2–10, 1973.

[28] J. Ahrens and S. Spors. Analytical driving functions for higher-order ambisonics. In *IEEE International Conference on Acoustics, Speech, and Signal Processing (ICASSP)*, 2008.

[29] J. Ahrens and S. Spors. Reproduction of a plane-wave sound field using planar and linear arrays of loudspeakers. In *Third IEEE-EURASIP International Symposium on Control, Communications, and Signal Processing*, 2008.

[30] M.A. Poletti. Three-dimensional surround sound systems based on spherical harmonics. *Journal of the AES*, 53(11):1004–1025, November 2005.

[31] S. Spors. Extension of an analytic secondary source selection criterion for wave field synthesis. In *123th AES Convention*, New York, USA, October 2007. Audio Engineering Society (AES).

[32] S. Spors. An analytic secondary source selection criteria for wave field synthesis. In *33rd German Annual Conference on Acoustics (DAGA)*, Stuttgart, Germany, March 2007.

[33] J. Ahrens and S. Spors. Implementation of directional sources in wave field synthesis. In *IEEE Workshop on Applications of Signal Processing to Audio and Acoustics*, New Paltz, USA, October 2007.

[34] E. Corteel. Synthesis of directional sources using wave field synthesis, possibilities, and limitations. *EURASIP Journal on Advances in Signal Processing*, 2007, 2007. Article ID 90509.

[35] Marije A.J. Baalman. Discretization of complex sound sources for reproduction with wave field synthesis. In *31. Deutsche Jahrestagung für Akustik*, Munic, Germany, 2005.

[36] S. Moreau, J. Daniel, and Bertet S. Reproduction of arbitrarily shaped sound sources with wave field synthesis - physical and perceptual effects. In *122th AES Convention*, Vienna, Austria, May 2007. Audio Engineering Society (AES).

[37] A. Franck, A. Gräfe, T. Korn, and M. Strauss. Reproduction of moving sound sources by wave field synthesis: An analysis of artifacts. In *32nd International AES Conference*, Hillerod, Denmark, September 2007. Audio Engineering Society (AES).

[38] J. Ahrens and S. Spors. Reproduction of moving virtual sound sources with special attention to the doppler effect. In *124th AES Convention*, Amsterdam, The Netherlands, April 2008. Audio Engineering Society (AES).

[39] S. Yon, M. Tanter, and M. Fink. Sound focusing in rooms: the time-reversal approach. *Journal of the Acoustical Society of America*, 113(3):1533–1543, March 2003.

[40] M. Fink. Time reversal of ultrasonic fields – Part I: Basic principles. *IEEE Transactions on Ultrasocics, Ferroelectrics, and Frequency Control*, 39(5):555–566, Sept. 1992.

[41] J. Ahrens and S. Spors. Notes on rendering of focused directional sound sources in wave field synthesis. In *34rd German Annual Conference on Acoustics (DAGA)*, Dresden, Germany, 2008.

[42] S. Spors and R. Rabenstein. Spatial aliasing artifacts produced by linear and circular loudspeaker arrays used for wave field synthesis. In *120th AES Convention*, Paris, France, May 2006. Audio Engineering Society (AES).

[43] M. Abramowitz and I.A. Stegun. *Handbook of Mathematical Functions*. Dover Publications, 1972.

[44] S. Spors. Spatial aliasing artifacts produced by linear loudspeaker arrays used for wave field synthesis. In *Second IEEE-EURASIP International Symposium on Control, Communications, and Signal Processing*, Marrakech, Morocco, March 2006.

[45] D. Leckschat and M. Baumgartner. Wellenfeldsynthese: Untersuchungen zu Alias-Artefakten im Ortsfrequenzbereich und Realisierung eines praxistauglichen WFS-Systems. In *31. Deutsche Jahrestagung für Akustik*, Munic, Germany, 2005.

[46] M.M. Boone, Verheijen E.N.G., and P. van Tol. Spatial sound-field reproduction by wave-field synthesis. *Journal of the AES*, 43(12), December 1995.

[47] S. Spors, M. Renk, and R. Rabenstein. Limiting effects of active room compensation using wave field synthesis. In *118th AES Convention*, Barcelona, Spain, May 2005. Audio Engineering Society (AES).

[48] H. Wittek. Perceptual enhancement of wave-field synthesis by stereophonic means. *Journal of the Audio Engineering Society*, 55(9), September 2007.

[49] E. Corteel, N. Khoa-Van, O. Warusfel, T. Caulkins, and R. Pellegrini. Objective and subjective comparison of electrodynamic and map loudspeakers for wave field synthesis. In *30nd International Conference on Intelligent Audio Environments*, Saarisekä, Finnland, March 2007. Audio Engineering Society (AES).

[50] S. Spors, A. Kuntz, and R. Rabenstein. An approach to listening room compensation with wave field synthesis. In *AES 24th International Conference on Multichannel Audio*, pages 49–52, Banff, Canada, June 2003. Audio Engineering Society (AES).

[51] S. Spors, A. Kuntz, and R. Rabenstein. Listening room compensation for wave field synthesis. In *IEEE International Conference on Multimedia and Expo (ICME)*, pages 725–728, Baltimore, USA, July 2003.

[52] S. Spors, H. Buchner, and R. Rabenstein. A novel approach to active listening room compensation for wave field synthesis using wave-domain adaptive filtering. In *IEEE International Conference on Acoustics, Speech, and Signal Processing (ICASSP)*, Montreal, Canada, 2004.

[53] S. Spors, H. Buchner, and R. Rabenstein. Adaptive listening room compensation for spatial audio systems. In *European Signal Processing Conference (EUSIPCO)*, 2004.

[54] S. Spors, H. Buchner, and R. Rabenstein. Efficient active listening room compensation for Wave Field Synthesis. In *116th AES Convention*, Berlin, Germany, 2004. Audio Engineering Society (AES).

[55] S. Petrausch, S. Spors, and R. Rabenstein. Simulation and visualization of room compensation for wave field synthesis with the functional transformation method. In *119th AES Convention*, New York, USA, 2005. Audio Engineering Society (AES).

[56] S. Spors and R. Rabenstein. Evaluation of the circular harmonics decomposition for WDAF-based active listening room compensation. In *28th AES Conference: The Future of Audio Technology – Surround and Beyond*, pages 134–149, Pitea, Sweden, June 2006. Audio Engineering Society (AES).

[57] J.J. Lopez, A. Gonzalez, and L. Fuster. Room compensation in wave field synthesis by means of multichannel inversion. In *IEEE Workshop on Applications of Signal Processing to Audio and Acoustics*, New Paltz, USA, Oct. 2005.

[58] R. von Zon, E. Corteel, D. de Vries, and O. Warusfel. Multi-actuator panel (map) loudspeakers: how to compensate for their mutual reflections? In *116th convention of the Audio Engineering Society*, Berlin, Germany, May 2004.

[59] P.-A. Gauthier and A. Berry. Sound-field reproduction in-room using optimal control techniques: Simulations in the frequency domain. *Journal of the Acoustic Society of America*, 117(2):662–678, Feb. 2005.

[60] P.A. Gauthier and A. Berry. Adaptive wave field synthesis with independent radiation mode control for active sound field reproduction: Theory. *Journal of the Acoustical Society of America*, 119(5):2721–2737, May 2006.

[61] E. Corteel and R. Nicol. Listening room compensation for wave field synthesis. What can be done? In *23rd AES International Conference*, Copenhagen, Denmark, May 2003. Audio Engineering Society (AES).

[62] E. Corteel, U. Horbach, and R.S. Pellegrini. Multichannel inverse filtering of multiexciter distributed mode loudspeakers for wave field sythesis. In *112th AES Convention*, Munich, Germany, May 2002. Audio Engineering Society (AES).

[63] A. Kuntz and R. Rabenstein. An approach to global noise control by wave field synthesis. In *European Signal Processing Conference (EUSIPCO)*, Vienna, Austria, Sept. 2004.

[64] S. Spors and H. Buchner. An approach to massive multichannel broadband feedforward active noise control using wave-domain adaptive filtering. In *IEEE Workshop on Applications of Signal Processing to Audio and Acoustics*, New Paltz, USA, October 2007.

[65] S. Spors and H. Buchner. Efficient massive multichannel active noise control using wave-domain adaptive filtering. In *Third IEEE-EURASIP International Symposium on Control, Communications, and Signal Processing*, 2008.

[66] P. Peretti, S. Cecchi, L. Palestini, and F. Piazza. A novel approach to active noise control based on wave domain adaptive filtering. In *IEEE Workshop on Applications of Signal Processing to Audio and Acoustics*, New Paltz, USA, Oct. 2007.